Published in final edited form as:
Ann Neurol. 2013 February ; 73(2): 266–280. doi:10.1002/ana.23788.

DIGESTION PRODUCTS OF THE PH20 HYALURONIDASE INHIBIT REMYELINATION

Marnie Preston, Ph.D.[1], **Xi Gong, M.D.**[2], **Weiping Su, M.D., Ph.D.**[1], **Steven G. Matsumoto**[1,3], **Fatima Banine, Ph.D.**[1], **Clayton Winkler, B.S.**[1], **Scott Foster, B.S.**[1], **Rubing Xing, B.S.**[1], **Jaime Struve, B.S.**[1], **Justin Dean, Ph.D.**[2], **Bruce Baggenstoss, B.S.**[4], **Paul H. Weigel, Ph.D.**[4], **Thomas J. Montine, M.D., Ph.D.**[5], **Stephen A. Back, M.D., Ph.D.**[2,6], and **Larry S. Sherman, Ph.D.**[1,7]

[1]Division of Neuroscience, Oregon National Primate Research Center, Beaverton, OR

[2]Department of Pediatrics, Oregon Health & Science University, Portland, OR

[3]Integrative Bioscience Department, School of Dentistry, Oregon Health & Science University

[4]Department of Biochemistry and Molecular Biology and the Oklahoma Center for Medical Glucobiology, University of Oklahoma Health Sciences Center, Oklahoma City, OK

[5]Department of Pathology, University of Washington, Seattle, WA

[6]Department of Neurology and Cell, Oregon Health & Science University, Portland, OR

[7]Department of Developmental Biology, Oregon Health & Science University, Portland, OR

Abstract

OBJECTIVE—Oligodendrocyte progenitor cells (OPCs) recruited to demyelinating lesions often fail to mature into oligodendrocytes (OLs) that remyelinate spared axons. The glycosaminoglycan hyaluronan (HA) accumulates in demyelinating lesions and has been implicated in the failure of OPC maturation and remyelination. We tested the hypothesis that OPCs in demyelinating lesions express a specific hyaluronidase, and that digestion products of this enzyme inhibit OPC maturation.

METHODS—Mouse OPCs grown *in vitro* were analyzed for hyaluronidase expression and activity. Gain of function studies were used to define the hyaluronidases that blocked OPC maturation. Mouse and human demyelinating lesions were assessed for hyaluronidase expression. Digestion products from different hyaluronidases and a hyaluronidase inhibitor were tested for their effects on OPC maturation and functional remyelination *in vivo*.

RESULTS—OPCs demonstrated hyaluronidase activity *in vitro* and expressed multiple hyaluronidases including HYAL1, HYAL2, and PH20. HA digestion by PH20 but not other hyaluronidases inhibited OPC maturation into OLs. In contrast, inhibiting HA synthesis did not influence OPC maturation. PH20 expression was elevated in OPCs and reactive astrocytes in both rodent and human demyelinating lesions. HA-digestion products generated by the PH20 hyaluronidase but not another hyaluronidase inhibited remyelination following lysolecithin-induced demyelination. Inhibition of hyaluronidase activity lead to increased OPC maturation and promoted increased conduction velocities through lesions.

INTERPRETATION—We determined that PH20 is elevated in demyelinating lesions and that increased PH20 expression is sufficient to inhibit OPC maturation and remyelination.

Correspondence to: Larry S. Sherman, Ph.D., Division of Neuroscience, Oregon National Primate Research Center, 505 NW 185th Avenue, Beaverton, OR 97006, Phone: (503) 690-5217; FAX: (503) 690-8534; shermanl@ohsu.edu.

Pharmacological inhibition of PH20 may therefore be an effective way to promote remyelination in multiple sclerosis and related conditions.

Demyelination occurs following numerous insults to the CNS and is the hallmark of multiple sclerosis (MS), causing conduction deficits that compromise motor, sensory and cognitive functions. Some recovery of function is associated with the recruitment of oligodendrocyte progenitor cells (OPCs) to demyelinating lesions, generating oligodendrocytes (OLs) that remyelinate spared axons.[1] However, OPCs often accumulate in chronically demyelinated lesions and fail to give rise to myelinating OLs.[2–7] Strategies that promote OPC maturation within demyelinating lesions therefore have the potential to promote remyelination and functional recovery in affected individuals.

Multiple signals within the microenvironments of demyelinating lesions contribute to the failure of OPC maturation and remyelination.[8, 9] We previously found that high molecular weight (HMW) forms of the glycosaminoglycan hyaluronan (HA) are among these signals. HA is synthesized by transmembrane synthases and is composed of multiple disaccharide units of glucuronic acid and *N*-acetylglucosamine. HA molecules range in size from $\leq 2.5\times10^5$ Da to $\geq 4\times10^6$ Da. Different molecular weight forms of HA have distinct functions in the nervous system including the regulation of cell motility, growth, and differentiation.[10, 11] We found that HA accumulates coincident with astrogliosis in demyelinating MS lesions,[12] traumatic spinal cord injuries,[13] perinatal white matter injuries,[14] lesions associated with vascular cognitive impairment[15] and during normal aging.[16] HA blocks OPC maturation and remyelination in lysolecithin-induced demyelinating lesions, suggesting that HMW HA accumulation contributes to remyelination failure.[12]

We reasoned that one strategy to promote remyelination within demyelinating lesions is to degrade accumulated HMW HA using hyaluronidases. During inflammatory responses outside the central nervous system (CNS), activated fibroblasts or other cells secrete hyaluronidases that degrade HA, generating HA digestion products that act as immune regulators.[17] Reactive oxygen species at sites of inflammation further promote this degradation.[18] Although hyaluronidases are expressed in the CNS,[19, 20] it is unclear if HA is similarly degraded at extracellular sites of CNS inflammation where astrocytes are the principle source of HA.[21]

Paradoxically, we and others have found that the digestion of HMW HA by some hyaluronidases prevents OPC maturation. A recent study found that treatment of OPCs with HA degraded by a combination of hyaluronidases and β-glucuronidase blocked OPC maturation *in vitro* through a mechanism involving toll-like receptor-2 (TLR2).[20] This study also demonstrated that lower MW forms of HA accumulate in MS lesions, that OPCs *in vitro* express multiple hyaluronidases, and that a broad spectrum hyaluronidase inhibitor can promote OPC maturation *in vitro.* The focus of the present study was to determine if hyaluronidases are expressed in human and rodent demyelinating lesions; if specific hyaluronidases alone can block OPC maturation; and if blocking hyaluronidase activity can promote remyelination *in vivo*.

Here, we report that an extracellular hyaluronidase, called PH20, is elevated in rodent and human demyelinating lesions. We demonstrate that PH20 expression is elevated in OPCs and astrocytes in chronic demyelinated MS lesions and in acute lesions in mice with experimental autoimmune encephalomyelitis (EAE). Elevated expression of PH20, but not other hyaluronidases, is sufficient to block OPC maturation. Digestion products of PH20, but not those generated by another hyaluronidase, potently block remyelination *in vivo*. Furthermore, inhibiting HA synthesis does not influence OPC maturation but blocking

hyaluronidase activity promotes OPC maturation and remyelination. Collectively, these data suggest that PH20 is a potential therapeutic target to promote remyelination.

Methods

Reagents

HMW HA (100 μg; 1.59×10^6 Da, Seigaku) was dissolved in sterile PBS and HA fragments were generated with addition of bovine testicular hyaluronidase (BTH; Sigma, 100 U/ml), *Streptomyces* hyaluronidase (StrepH; Sigma, 1–10 U/ml) or PBS vehicle for 1 hour at 37°C then incubated at 95–100°C for 30 minutes to heat inactivate enzymes. Digestions were evaluated by electrophoresis on a 0.5% agarose gel, followed by detection of HA using the cationic dye Stains-All (Sigma) as previously described.[22] 4-methylumbelliferone (4-MU; Sigma) was dissolved in PBS at 37°C and added to cultures at a final concentration of 0.1–1 mM. VCPAL (Sigma) was dissolved in DMSO at a concentration of 100 mM and further diluted to a working concentration of 2.5–25μM for cell culture experiments and for co-injection into lysolecithin lesions. Turbidity assays for VCPAL activity and IC_{50} calculations were performed as previously described.[23]

Analysis of HA size and concentration

HA concentration, size distribution, and weight-average molar mass (*Mw*) were determined by size exclusion chromatography-multiangle laser light scattering (SEC-MALLS) as previously described[24] using PL Aquagel-OH 60, 40, and 20 (Polymer Labs) size exclusion columns in series. MALLS analyses of the SEC column eluate was performed in line using a Dawn DSP Laser Photometer in series with an Optilab DSP Interferometric Refractometer (both from Wyatt Technologies). Data were analyzed using ASTRA version 4.73, a dn/dc value of 0.153 ml/g and first-order Berry fits.

Lentiviral Construction and Infections

The expression vector (LV-intron-GFP) used for cloning is from Gregory A. Dissen (Oregon National Primate Research Center, Beaverton, Oregon).[25] *PH20* and *Hyal5* cDNAs were obtained from Stephan Reitinger (Institute for Biomedical Aging Research, Austrian Academy of Sciences, Innsbruck, Austria). The *Hyal1* cDNA was from Barbara L. Triggs-Raine (University of Manitoba, Canada).[26] *Hyal2* was obtained by RT-PCR using the forward primer: 5′-GAGTTCCTGAGCTGCTACCA-3′ and the reverse primer: 5′-AGGGGGAGAGATCCCTCATA-3′. The open reading frame of *PH20*, *Hya1*, *Hyal2* and *Hyal5* were cloned in front of the CMV promoter of a vector plasmid and packaged into a third generation lentiviral vector. Cells were plated at $4–5 \times 10^4$ cells per coverslip and infected overnight using $2.5 –5.0 \times 10^5$ transforming units (MOI 1:50–1:100).

Cell Culture

Neural stem cells were isolated from the medial and lateral ganglionic eminences of embryonic day 13.5 mouse (C57BL/6) embryos and expanded in epidermal growth factor and fibroblast growth factor-2 (both at 10 ng/ml) as neurospheres for one week as previously described.[27] To generate OPCs, neurospheres were dissociated into single cells in trypsin (0.05%, Invitrogen), washed in Dulbecco's Modified Eagle Medium (DMEM) plus 10% fetal bovine serum and plated at 5×10^6 cells/ml on uncoated polystyrene plates in DMEM/F12 media containing 0.1% bovine serum albumin (BSA), platelet-derived growth factor AA (PDGF-AA) and fibroblast growth factor-2 (FGF2) at 20 ng/ml each, B27 supplement minus vitamin A (GIBCO), N1 supplement (Sigma) and D-Biotin (10 nM, Sigma). Small adherent oligospheres formed and were passaged once a week after dissociation with Accutase (Invitrogen). After 2–3 weeks oligospheres were transferred to poly-L-ornithine-

coated 100 mm dishes. After 1–2 passages, highly enriched populations (>95%) of PDGFR-α+Olig2+O4-OPCs (as assayed by immunocytochemistry; see Supplementary Fig. 1 for example) were obtained and further propagated for *in vitro* experiments. For maturation experiments, OPCs were plated at $4–5\times10^4$ cells per coverslip and differentiated in DMEM/F12, 0.1% BSA, plus triiodothyronine (T3, 30 nM, Sigma) and N-acetyl-L-cysteine (NAC, Sigma) as previously described.[27]

Lysolecithin Lesions

All animal experiments were approved by the Institutional Animal Care and Use Committee at the Oregon Health & Science University. Demyelination was induced in the rostral corpus callosum of 3–4 month old C57BL/6J mice by injection of lysolecithin (4% in PBS; Sigma) as previously described[12] mixed with either vehicle (PBS), HMW HA, degraded HA, or VCPAL. Five days post-lysolecithin injection, the same volumes of PBS, HA, or VCPAL were re-injected. Brains were harvested at 8-days post-lysolecithin injection, fixed and processed for immunohistochemistry as previously described.[12]

Induction of EAE

EAE was induced in female C57BL/6J mice as previously described.[12] Animals were anesthetized with isofluorane and perfused transcardially with 100 U/ml sodium heparin (Sigma-Aldrich) containing saline followed by 4% paraformaldehyde in PBS. Spinal cords were dissected and processed for immunohistochemistry as described below.

Immunohistochemistry

Cells were fixed for 30 minutes at room temperature in 4% paraformaldehyde and washed 3 times in PBS. Lumbar spinal cord tissue from mice with EAE was immersion fixed for 12–16 hrs in 4% paraformaldehyde at 4°C, rinsed three times in PBS at room temperature, then cyroprotected in 30% sucrose overnight at 4°C. Tissues were embedded in Optimal Cutting Temperature (OCT) medium, rapidly frozen on dry ice and cryosectioned at a thickness of 10–12 μm. Cells and tissues were pre-blocked in 10% heat-inactivated fetal bovine serum for 45 minutes. Primary antibodies were diluted in blocking buffer and cells or EAE tissue were incubated overnight at 4°C, rinsed in blocking buffer three times, then incubated with the appropriate species-specific fluoro-conjugated secondary antibodies (Alexa546 or Alexa488, Molecular Probes Inc.) for 45 minutes. Antibodies used were: rat anti-PDGFR-α (1:250, BD Pharminagen), mouse anti-O4 (1:500, Millipore), mouse anti-myelin basic protein (MBP; 1:1000, Sternberger Monoclonal), rabbit anti-GalC (1:100, Millipore), rabbit anti-glial fibrillary acidic protein (GFAP; 1:1000, DAKO), rabbit anti-microtubule-associated protein-2 (MAP2; 1:1000, Millapore), and rabbit anti-Olig2 (1:500, Millipore). Polyclonal rabbit antisera to PH20 were generously provided by James Overstreet (PH20, 1:1000) and Patricia DeLeon (msSPAM, 1:400). HA was visualized by probing cells or tissues with biotinylated HA Binding Protein (HABP, 1:200, Seikagaku) followed by avidin-conjugated Cy3 (1:1000, Molecular Probes Inc.). Myelin was visualized by a 30-minute incubation of EAE sections with Fluoromyelin (1:400 in PBS, Invitrogen) following primary and secondary antibody application. Cell nuclei were visualized by DAPI staining (Hoeschst 33342, 1:15,000; Molecular Probes). Sections from mice with lysolecithin lesions were analyzed for MBP reactivity as previously described.[12]

The use of tissues from individuals with MS was approved by the Human Subjects Committee at the University of Washington. For the analysis of MS patient lesions, paraffin sections from 5 MS patients (mean duration of disease: 16.4 years; mean age: 57.6 years; see Supplementary Table 1) were deparaffinized in xylene and then rehydrated in graded alcohols. Endogenous peroxidase activity was blocked with 0.3% (v/v) hydrogen peroxide in methanol before washing the slides in water. Slides were heated in citrate buffer (10 mmol/

L, pH 6.0) for 5 min in a microwave for antigen retrieval. Sections were then pre-blocked in 5% normal goat serum. Primary antibody incubation was the same as indicated above, except that rabbit anti PH20 (J. Overstreet) was used at a 1:500 dilution. Following biotinylated goat anti-rabbit secondary antibody binding, the avidin–biotin–peroxidase complex technique (Vectastain ABC kit and NovaRED, Vector Laboratories Inc.) was used for visualization according to the manufacturer's instructions. In separate experiments, sections were also double-labeled with anti-PH20 (1:300) and either anti-MBP (1:500), anti-O4 (1:400), or anti-GFAP (1:50, DAKO) followed by fluorescence-conjugated secondary antibodies as above.

Image processing and cell counts were performed using Photoshop 3.0 and ImageJ, respectively. For cell counts, 10 fields were randomly selected and at least 500 cells counted per coverslip (3 coverslips per group). Mean cell numbers and standard deviations were calculated for each group.

Quantitative analysis of OPC maturation in lysolecithin-induced lesions

Serial tissue sections (50 μm) were cut on a vibrating microtome (Leica VTS-1000). Tissue sections were double-labeled for CC-1 (mature OL marker) and PDGFR-α (OL progenitor marker) and counterstained with Hoechst 33324. Tissue sections were first treated for antigen retrieval (10 minutes at 95°C in 50 mM Tris-EDTA buffer, pH 9.0). Tissue was incubated at 4°C for 3 days with a mouse monoclonal antibody CC-1 (OP80, 1:200 in PBS with 0.1% triton X-100, Calbiochem) and a rabbit polyclonal antisera against PDGFR-α (1:500, in PBS with 0.1% triton X-100; a generous gift of Dr. William Stallcup, Burnham Institute, La Jolla, CA). Sections were also stained with DAPI to identify cell nuclei. Cell counts within LYS-induced lesions were performed using a 40x objective with a counting radicle mounted on a Leica DMRA epifluorescence microscope. Cell counts were done in three separate zones that corresponded to a central region of chronic demyelination (Zone 1), an adjacent region of active remyelination (Zone 2) and the most lateral zone, which was equivalent to normal surrounding white matter (Zone 3). For each study, a minimum of 5 animals was analyzed and counts were obtained from duplicate adjacent sections. Given the irregular shape of the lesions it was not feasible to precisely define the boundaries of these three zones. Each zone displayed a unique pattern of nuclear cell density that allowed it to be readily distinguished from adjacent zones. Zone 1 typically had a very high density of cell nuclei, whereas zone 2 had a density that was intermediate between zones 1 and 3. Within each zone, cell counts were done in a standardized number of fields that maximized the number that could be defined: zone 1 (2 fields), zones 2 and 3 (6 fields each).

Compound action potential (CAP) recordings

Brains were rapidly removed and submerged in ice cold artificial cerebrospinal fluid (aCSF; 124 mM NaCl, 5 mM KCl, 1.25 mM NaH_2PO_4, 26 mM $NaHCO_3$, 1.3 mM $MgSO_4$, 2 mM $CaCl_2$, 10 mM glucose, pH 7.4) saturated with 95% O_2/5% CO_2. A 400 μm thick coronal slice corresponding to Bregma coordinates 0.5 to 0.9 was cut on a vibratome (Leica), collected and incubated in aerated aCSF at room temperature for 1 hour prior to recording.

For recording, the slice was transferred to a perfusion chamber mounted on an upright microscope (Zeiss). The tract of the injection electrode was usually visible, however, injection sites were confirmed with subsequent histochemical analysis of the slice. Recording and stimulating electrodes were positioned in the corpus callosum on the side of the injection and then moved to the opposite side to obtain recordings of untreated axons. The bipolar stimulating electrodes were fashioned from teflon-insulated tungsten wires (WPI) with tips positioned approximately 0.3 mm apart. The stimulating electrodes were connected to a stimulator (Grass S88) and stimulation isolation unit (Grass). Stimulus

intensity was adjusted to obtain a maximal response. Recordings were obtained using glass microelectrodes filled with aCSF with a resistance of 3–5 Megaohm. Recordings were amplified and filtered at 10 kHz. Recordings were obtained from 2 sites across the width of the corpus callosum at approximately 1.5 mm from the stimulating electrode. Ten responses were averaged at each recording site. The magnitude of the CAP waveform was determined by measuring the maximum negative deflection with respect to a tangent drawn between the adjacent positive deflections. For each recording session 3 animals per group (treated with VCPAL or vehicle) were analyzed.

RT-PCR and qRT-PCR

Total RNA was isolated from cells or tissues using Trizol (Invitrogen) following the manufacturer's instructions. mRNA was reverse transcribed into cDNA using random hex or oligo d(t) primers and a reverse transcriptase kit (Promega). mRNA sequences for each hyaluronidase were downloaded from the NCBI website (http://www.ncbi.nlm.nih.gov) and primers for RT-PCR were designed manually (supplied by Intergrated DNA Technologies). See Supplementary Table 2 for primers used. RT-PCR was performed using GoTaq or Superscript DNA transcriptase (Promega or Invitrogen) in a Mastercycler Gradient (Eppendorf) following the manufacturer's protocols. RT-PCR reaction products were analyzed by electrophoresis on a 1% agarose gel and amplicons visualized following staining with ethidium bromide. Quantitative Real Time PCR (qRT-PCR) was performed using predesigned primer and probe sets (Taqman Assays, Applied Biosciences; HYAL1: Mm00476206; HYAL2: Mm0477731; and PH20 (SPAM1): Mm00486329, with an AB 7900HT fast PCR system using SDS 2.4 software. Data Analysis was performed using Microsoft Excel.

Statistics

An unpaired two-tailed t-test was used to compare changes in anti-PDFGFR-α- and anti-MBP immunolabeled cells in *in vitro* experiments. One-way analysis of variance (ANOVA) followed by Tukey's multiple comparison test was used to assess changes in the percentages, relative to controls, of mature OL's in cultures treated with VCPAL and for the analysis of qRT-PCR experiments. A value of $p < 0.05$ was considered significant.

Results

A specific hyaluronidase blocks OPC maturation in vitro

We previously found that HMW forms of HA accumulate in demyelinating lesions and that the presence of HA blocks OPC maturation and remyelination.[12] Sloane and co-workers[20] reported that HMW HA digested by a combination of a hyaluronidase and β-glucuronidase blocked OPC maturation *in vitro*. To further explore the role of HA in OPC maturation, we utilized a culture system in which mouse neural stem cells are differentiated *in vitro* into mouse OPCs (>90% PDGFR-α^+/$O4^-$/$GalC^-$/MBP^- cells) that can subsequently generate pre-OLs ($O4^+$/$GalC^-$/MBP^- cells) and mature OLs (MBP^+ cells) in the presence of a pro-differentiation medium that contained T3 and NAC (Supplementary Fig. 1A–F). After 3 hours in culture, we observed elevated peri-cellular HA synthesis by OPCs that increased over time (Supplementary Fig. 2A–C). HA synthesis continued to accumulate in pre-OL cultures 24 hours following T3 and NAC treatment, but then diminished in cultures enriched with MBP^+ cells, with HA remaining associated with cell bodies (Supplementary Fig. 2D, E). All three HA synthases were expressed by OPC cultures (Supplementary Fig. 2F).

Although as many as 60% of cells in these mouse OPC cultures became MBP+ OLs in pro-differentiation medium, approximately 40% of cells consistently failed to mature (Fig. 1). We hypothesized that the low level of HA synthesized in our cultures was sufficient to block

the maturation of a limited number of OPCs. We therefore tested if the prevention of HA synthesis is sufficient to increase OL maturation in these cultures. To block HA synthesis, OPCs were switched to media containing the HA synthase inhibitor 4-methylumbelliferone (4-MU). HA synthesis was almost completely blocked by 1 mM 4-MU (Fig. 1A, B). Unexpectedly, we found that inhibiting HA synthesis had no significant effect on OL maturation compared to controls despite the nearly complete absence of HA in these cultures (Fig. 1D, E, G).

We next tested if degradation of HA could influence OPC maturation. In contrast to the results of Sloane and co-workers,[20] we found that bovine testicular hyaluronidase (BTH) alone at concentrations between 25 and 100 U/ml completely degraded HA in OPC cultures (Fig. 1C) and inhibited OPC maturation (Fig. 1F, G). This inhibitory activity was reversed by heat inactivation of the enzyme prior to HA digestion (data not shown). OPC maturation was not inhibited when cultures were treated with *Streptomyces* hyaluronidase (StrepH) or with chondroitinase ABC (which degrades chondroitin sulfate into unsaturated disaccharides) at concentrations that were optimal for the digestion of HA and chondroitin sulfate, respectively (Fig. 1H). This finding is consistent with the hypothesis that specific HA digestion products are capable of inhibiting OPC maturation *in vitro*.

The PH20 hyaluronidase, but not other hyaluronidases, potently inhibits OPC maturation

The soluble hyaluronidase activity in BTH has been attributed to the PH20 enzyme.[28] We therefore performed gain-of-function experiments to test how increased expression of PH20 and other mammalian hyaluronidases influenced OPC maturation. The cDNAs from mouse *Hyal1*, *Hyal2*, *Hyal5* and *PH20* were cloned into a bicistronic lentiviral expression vector carrying the cDNA for enhanced green fluorescence protein (EGFP). OPCs were then infected with lentiviruses carrying each construct and analyzed for changes in OPC maturation as described above. OPC cultures infected with the control virus, carrying EGFP alone, demonstrated pericellular HA accumulation (Fig. 2A) while HA was reduced in cultures infected with the *PH20* (Fig. 2B) and the *Hyal1*, *Hyal2*, and *Hyal5* viruses (data not shown). Cells infected with the PH20-carrying virus demonstrated a significant ($p<0.0009$) and pronounced inhibition of OPC maturation (Fig. 2D, E) as assessed by quantification of MBP+ cells, compared to cultures infected with a virus carrying only the EGFP cDNA (38% of control; Fig. 2C, E). Infection with the *Hyal1*-bearing virus had no significant effect on OL maturation while cells infected with viruses carrying *Hyal2* and *Hyal5* only weakly inhibited OL maturation (approximately 80% and 73% of control, respectively; $p<0.02$; Fig. 2E).

HA digestion products generated by PH20 are sufficient to inhibit remyelination in vivo

Taken together, our data support the hypothesis that specific HA digestion products generated by PH20 but not other hyaluronidases or chondroitinase potently inhibit OPC maturation. To determine if PH20 generates distinct HA degradation products, we analyzed HMW HA that had been treated with either PH20 (BTH) or StrepH using the quantitative and sensitive SEC-MALLS technique to characterize the HA products in these two digests (Fig. 3A). The weight-average sizes of the PH20 (63.9 ± 0.5 kDa) and StrepH (2.4 ± 0.4 kDa) digests were very different. More importantly, the two distributions of HA product sizes in the two digests were essentially not overlapping. Only about 2% of the products in both digests were in the same size range (e.g. 98% of the PH20 products ranged from 5.5 to 227 kDa and 98% of the StrepH products were < 4.4 kDa).

We next determined whether the HA digestion products generated by PH20 activity were capable of blocking remyelination. We induced focal demyelination in the corpus callosum of mice using lysolecithin as previously described.[12] After 5 days, a second injection of

either vehicle, HMW HA that had been incubated with vehicle, PH20-degraded HMW HA, or StrepH-degraded HMW HA was delivered into the original lesion site. Brains from these animals were analyzed 8 days after the initial lysolecithin injection ($n \geq 6$ per group). OPC maturation was assessed by analysis of MBP immunoreactivity in sections through lesions as previously described.[12] As expected, elevated MBP immunoreactivity at the sites of lesions was observed in animals injected with vehicle (Fig. 3B). Consistent with our previous findings[12] MBP expression was reduced in lesions injected with HMW HA (Fig. 3C shows typical example). MBP expression was also reduced in lesions injected with PH20-digested HA (Fig. 3D), but was comparable to vehicle-injected controls in animals treated with StrepH-digested HA (Fig 3E).

To further characterize and quantify the effects of PH20-digested HA on OPC maturation, we analyzed the proportion of cells within lesions ("zone 1"), at lesion borders ("zone 2"), and in adjacent unaffected white matter ("zone 3") that express PDGFR-α and CC1 (a marker of mature OL cell bodies) in lysolecithin-induced demyelinated lesions (Supplementary Fig. 3) after 8 days as above. We observed a significant increase in PDGFR-α^+ and CC1+ cells within lesions compared to unaffected white matter (Fig. 3F, G), consistent with the idea that OPCs are recruited to demyelinating lesions and mature into OLs that remyelinate spared axons. Interestingly, we did not observe increased numbers of PDGFR-α^+ cells at lesion borders, but there was a significant increase in the numbers of CC1+ cells at borders. The lesion borders are similar to so-called shadow plaques where partial remyelination occurs. It is possible, therefore, that the increased numbers of OLs at the borders of lesions are the result of increased OPC maturation due to a lack of inhibitory signals in this location. Adding PH20-induced HA digestion products to lesions resulted in a significant increase in PDGFR-α^+ cells and a significant decrease in CC1+ cells (Fig. 3F, G), indicating that OPCs were still recruited to lesions but failed to mature into OLs. Specific HA-digestion products produced by PH20 are therefore capable of blocking OL maturation in demyelinated lesions *in vivo*.

OPCs express hyaluronidases and degrade HA

A previous study using only immunohistochemistry with single antibodies reported that OPCs *in vitro* express multiple hyaluronidases, including PH20.[20] Other reports, however, had indicated that PH20 was localized to testes but not other tissues.[29–32] To confirm that PH20 is expressed by OPCs, we isolated total RNA from mouse testes (as a positive control for testicular hyaluronidases), from OPCs grown *in vitro*, and from adult mouse corpus callosum, then performed RT-PCR using primers specific for the hyaluronidases with known hyaluronidase activity in mouse testes (Hyal1 Hyal2, Hyal5 and PH20). We found that Hyal1, Hyal2 and PH20 but not the testes-specific Hyal5 were expressed by OPCs and in white matter using both RT-PCR (Fig. 4) and qRT-PCR (data not shown). Hyal1, Hyal2 and PH20 transcripts were also amplified from RNA isolated from whole brain, cortex and spinal cord (data not shown). To verify that the transcripts we had amplified by RT-PCR were indeed PH20, three distinct sets of primers (Supplementary Table 2) were used to amplify separate regions of PH20 mRNA isolated from adult mouse brain and were sequenced, confirming that OPCs express bona fide PH20 RNA (data not shown).

Given that PH20 transcripts are expressed by OPCs and in the corpus callosum, and that elevated PH20 expression is sufficient to inhibit OPC maturation, we examined PH20 expression in OL lineage cells at different stages of differentiation. PH20 protein expression was assayed in proliferating OPCs and maturing OLs by immunocytochemistry using two separate PH20 antibodies (generous gifts of P. DeLeon and J. Overstreet) in combination with the OL lineage specific markers PDGFR-α, O4 or MBP. PH20 immunostaining localized both to the cell body and processes of immature PDGFR-α+ OPCs (Fig. 5A–D). In contrast, PH20 was highly enriched in the cell body and in the tips of processes in O4+ pre-

OLs (Fig. 5E–H). PH20 expression was reduced in mature MBP+ OLs where it became restricted to the cell body (Fig. 5I–L). All together, these data indicate that the distribution of PH20 is maturation-dependent and becomes reduced in processes and restricted to the cell body as OPCs mature into OLs.

Because PH20 is a GPI-anchored hyaluronidase that can function at neutral pH, we reasoned that its expression by OPCs would lead to the digestion of extracelluar HA. We therefore determined if OPCs are capable of degrading HA. OPCs were plated onto coverslips uniformly coated with HMW HA (approximately 1.59 MDa), differentiation was promoted in the presence of T3 and NAC for 24 or 72 hours, then cells were fixed and labeled with an anti-O4 antibody and a biotinylated HA-binding protein (HABP). We observed a loss of HABP staining around the cell bodies and processes of O4+ cells at 24 hours *in vitro* (Fig. 6A–C). After 72 hours of OPC differentiation, O4 staining demonstrated membrane sheets of maturing OLs that were associated with a pronounced loss of HABP staining (Fig. 6D–F). Collectively, these data indicate that OL-lineage cells express PH20 and are capable of digesting extracellular HMW HA.

PH20 expression is elevated in demyelinating lesions

Because we found that HMW HA accumulates in chronic demyelinated lesions,[12] that PH20 expressed by OPCs can degrade HMW HA, and that PH20 breakdown products can inhibit OPC maturation and remyelination, we hypothesized that PH20 expression may be up-regulated in demyelinated lesions. In mice with EAE, we observed that PH20 was not detectable in unaffected adult white matter but was elevated in active, acute demyelinated spinal cord lesions (e.g., circled areas in Fig. 7A–D) where it was expressed by both reactive astrocytes and occasionally by OPCs (data not shown).

In chronically demyelinated plaques of MS patients (n=5; see Supplementary Table 1), PH20 immunoreactivity was enriched at the borders of lesions with only small numbers of immunoreactive cells in the center of lesions (Fig. 7E, arrows; Supplementary Fig. 4). Numerous cells expressed PH20 at the lesion borders (Fig. 7F). Double labeling immunohistochemistry revealed that the majority of these PH20+ cells originated from GFAP+ reactive astrocytes (Fig. 7G; arrows) as well as a subpopulation of O4+ pre-oligodendrocytes (Fig. 7H; arrows). HA staining was reduced in PH20-high areas in MS lesions, consistent with the finding that PH20+ OPCs can degrade extracellular HA (Supplementary Fig. 5). These data indicate that PH20 expression and activity are elevated in rodent and human demyelinating lesions.

Pharmacological inhibition of hyaluronidase activity promotes OL maturation and functional remyelination

Given that OPCs express multiple hyaluronidases and that degradation products of PH20 inhibit OPC maturation, we reasoned that blocking the activity of hyaluronidases, and therefore the generation of inhibitory HA breakdown products, would promote OL maturation. We chose to inhibit hyaluronidase activity in OPC cultures with the hyaluronidase inhibitor 6-O-Palmitoyl-L-ascorbic acid (VCPAL) for 72–96 hours. Consistent with previous studies, we found that VCPAL inhibited BTH/PH20 activity with an IC_{50} of 25–35 μM (Supplementary Fig. 6). We examined VCPAL-treated and control (vehicle) cultures for changes in the expression of the OL lineage markers PDGFR-α to label OPCs and MBP to label mature OLs. VCPAL treatment prevented HA degradation as assayed by HABP labeling (data not shown) and significantly increased the proportion of cells that became mature OLs, assayed as the total percentage of cells expressing MBP as compared to cultures treated with vehicle alone (Fig. 8A–C).

To assess whether inhibition of hyaluronidase activity is sufficient to promote OPC maturation *in vivo*, we co-injected VCPAL with HMW HA into lysolecithin-induced corpus callosum lesions. In animals with lysolecithin-induced lesions, VCPAL resulted in elevated MBP immunoreactivity (Fig. 8D–E; arrows) similar to that seen in animals injected with vehicle alone (e.g. Fig. 3B). When we quantified OPCs and mature OLs within lesions, at lesion borders, and in adjacent unaffected white matter as described above, we found that there was a trend towards increased numbers of CC1+ cells and decreased numbers of PDGFR-α^+ cells within lesions treated with HMW HA and VCPAL compared to controls injected with vehicle and HMW HA (Fig. 8F, G, zone 1). At lesion borders, VCPAL-treated animals demonstrated a significant increase in PDGFR-α^+ and CC1+ cells (Fig. 8F, G) indicating that VCPAL enhanced recruitment and maturation of OPCs, especially at lesion borders.

We next tested whether VCPAL could promote the functional remyelination of lysolecithin-induced lesions. Mice were treated as above with VCPAL or vehicle (n=3/group/experiment) and slices of corpus callosum that included the injection site were analyzed using compound action potential (CAP) recordings. Representative recordings of slices are shown in Fig. 9A–C. There was a lack of fast latency peaks (representing myelinated axons) in animals injected with HA and vehicle (Fig. 9A), but increased high latency peaks in animals that received VCPAL (Fig. 9B), similar to those observed in the control hemisphere (Fig. 9C). Following the recording, the 400 μm slices were fixed and immunolabeled as whole mounts for MBP. Immunolabeling verified increased MBP immunoreactivity in animals treated with VCPAL as compared to animals injected with vehicle (Fig. 9D, E). Quantification of high:low latency peak ratios (Fig. 9F) confirmed that VCPAL increased conduction velocities in the corpus callosum of mice treated with lysolecithin and HMW HA while treatment with vehicle had no affect on conduction velocities.

All together, these findings support the hypothesis that the hyaluronidase activity of OPCs and other cells in demyelinating lesions contributes to the impairment of OL maturation and thus to the remyelination failure seen in chronically demyelinated lesions and MS plaques. These data further suggest that inhibiting hyaluronidase activity, and particularly PH20 activity, may be an efficacious strategy to promote remyelination.

Discussion

We have demonstrated for the first time that the PH20 hyaluronidase is elevated in astrocytes and OPCs in demyelinating lesions from MS patients and rodents with EAE; that elevated expression of PH20 by OPCs is sufficient to inhibit OPC maturation; that HA digestion products generated by PH20 are sufficient to inhibit OPC maturation and remyelination; and that inhibiting hyaluronidase activity promotes OPC maturation and remyelination *in vivo*. Although an earlier study reported that a wide range of HA molecules with different molecular weights are present in demyelinating MS lesions,[20] our findings support the hypothesis that the molecules that inhibit OPC maturation and remyelination are a specific set of digestion products generated by PH20.

Previous studies from our group and others reported that HMW HA accumulates in demyelinating lesions and that adding HMW HA to demyelinated lesions prevents OPC maturation and remyelination.[12,20] Indeed, HA and HA receptors, including CD44 and TLR2, are elevated coincident with astrogliosis following a variety of CNS insults including demyelinating lesions in MS patients and mice with EAE,[12,20] traumatic spinal cord injuries,[13] and ischemia.[33] HA is also elevated in the brains of aged rodents[34] and non-human primates,[16] and in patients with Alzheimer's disease and age-related vascular brain injury.[15,35,36] Myelination disturbances occur in each of these conditions. Our data support a

model for remyelination failure whereby HMW HA is synthesized by reactive astrocytes and other cells within CNS lesions, the HA is degraded into specific HA digestion products by PH20 expressed by glial cells in the lesion microenvironment as well as OPCs recruited to lesions, and these HA digestion products in turn inhibit OPC maturation. The HMW HA added to demyelinating lesions in previous studies was therefore likely digested by PH20 expressed within lesions, and these digestion products and not HMW HA itself blocked remyelination. Thus, inhibiting hyaluronidase activity or blocking signaling by hyaluronidase-generated HA digestion products are potentially efficacious strategies for promoting remyelination in numerous conditions.

Our finding that PH20 expression in OPCs is localized to the tips of cell processes and then is restricted to the cell body in more differentiated OLs suggests that PH20 may play a role in regulating OPC-axon interactions during myelination. Thus, although PH20 digestion products inhibit OPC maturation and remyelination, and blocking PH20 activity promotes OPC maturation *in vitro*, the enhanced remyelination we observed following treatment with a hyaluronidase inhibitor could be the result of altering the regulated interactions between OPC processes and axons. Additional studies will be required to test this hypothesis.

HA digestion products may influence OPC maturation through a number of mechanisms. A study in Xenopus tadpoles demonstrated that glycogen synthase kinase-3b (GSK3β), a serine/threonine protein kinase that is part of the Wnt signaling cascade, is activated by HA signaling.[37] The Wnt signaling cascade and GSK3β in particular has been implicated in regulating OPC maturation.[38–41] Inhibition of GSK3β stimulates remyelination in adult mice.[40] It is possible therefore that HA digestion products inhibit OPC maturation at least in part through the activation of GSK3β. HA digestion products may also signal through TLR2 or TLR4,[42–46] both of which can also influence GSK3β activation.[47–48] Toll-like receptors are expressed by OPCs and one study has suggested that HA-mediated inhibition of OPC maturation is dependent on TLR2.[20] The contributions of other HA receptors, including CD44 and the receptor for hyaluronan-mediated motility, in regulating OPC maturation have yet to be elucidated.

HA digestion products likely act in concert with other signals in demyelinated lesions to prevent remyelination. Like HA accumulation, many of these signals appear to be linked to reactive astrogliosis. Reactive astrocytes in spinal cord injuries increase their expression of bone morphogenetic proteins that inhibit OPC differentiation with concurrent promotion of astrocyte differentiation.[49] It is possible that HA, which is synthesized predominantly by reactive astrocytes, acts on OPCs following its digestion by PH20 in concert with these and other inhibitory mechanisms including the NOGO receptor interacting protein LINGO-1 to prevent remyelination. [50]

Although we have demonstrated that inhibiting hyaluronidase activity is sufficient to promote remyelination in lesions where HA accumulates, such broad-acting inhibitors are not likely to be useful as therapeutic agents. Hyal1 and Hyal2, for example, are widely distributed in many different tissues.[51] *Hyal1*-null mice develop osteoarthritis[52] while humans with *HYAL1* mutations develop a lysosomal storage disorder, mucopolysaccharidosis (MPS) IX.[53] *Hyal2*-null mice develop skeletal and hematological abnormalities.[54] In contrast, although PH20 mRNA has been detected at high levels in testis and at low abundance in a limited number of other tissues, *PH20*-null mice do not display any significant pathological phenotypes.[55] Our finding that PH20 is specifically up-regulated in demyelinating lesions and is sufficient to block OPC maturation suggests that agents that target PH20 and not other hyalurondiases may be both safe and efficacious as long-term therapies for the promotion of remyelination.

Supplementary Material

Refer to Web version on PubMed Central for supplementary material.

Acknowledgments

We thank Dr. Patricia DeLeone and Dr. James Overstreet for PH20 antibodies and Ms. Louise Sacha for administrative assistance. This work was supported by National Institutes of Health grants NS056234 (LSS), NS054044, NS045737-06S1/06S2 (SAB), core grant RR00163 (LSS) supporting the Oregon National Primate Research Center and grant P30-NS061800 (LSS) supporting the imaging core at the Oregon National Primate Research Center; grant SRA-10-055 from Fast Forward, LLC (LSS), grant W81XWH-10-1-0967 from the Congressionally Directed Research Programs Multiple Sclerosis Research Program (LSS and PHW); The Laura Fund for Multiple Sclerosis Research (MP) and grants from the March of Dimes Birth Defects Foundation and the American Heart Association (SAB).

References

1. Franklin RJ, Ffrench-Constant C. Remyelination in the CNS: from biology to therapy. Nat Rev Neurosci. 2008; 9(11):839–855. [PubMed: 18931697]
2. Wolswijk G. Chronic stage multiple sclerosis lesions contain a relatively quiescent population of oligodendrocyte precursor cells. J Neurosci. 1998; 18(2):601–609. [PubMed: 9425002]
3. Scolding N, Franklin R, Stevens S, Heldin CH, Compston A, et al. Oligodendrocyte progenitors are present in the normal adult human CNS and in the lesions of multiple sclerosis. Brain. 1998; 121(Pt 12):2221–2228. [PubMed: 9874475]
4. Chang A, Nishiyama A, Peterson J, Prineas J, Trapp BD. NG2-positive oligodendrocyte progenitor cells in adult human brain and multiple sclerosis lesions. J Neurosci. 2000; 20(17):6404–6412. [PubMed: 10964946]
5. Maeda Y, Solanky M, Menonna J, Chapin J, Li W, et al. Platelet-derived growth factor-alpha receptor-positive oligodendroglia are frequent in multiple sclerosis lesions. Ann Neurol. 2001; 49(6):776–785. [PubMed: 11409430]
6. Chang A, Tourtellotte WW, Rudick R, Trapp BD. Premyelinating oligodendrocytes in chronic lesions of multiple sclerosis. N Engl J Med. 2002; 346(3):165–173. [PubMed: 11796850]
7. Wolswijk G. Oligodendrocyte precursor cells in the demyelinated multiple sclerosis spinal cord. Brain. 200; 125(Pt 2):338–349. [PubMed: 11844734]
8. Kotter MR, Stadelmann C, Hartung HP. Enhancing remyelination in disease--can we wrap it up? Brain. 2011; 134(Pt 7):1882–1900. [PubMed: 21507994]
9. Kremer D, Aktas O, Hartung HP, Küry P. The complex world of oligodendroglial differentiation inhibitors. Ann Neurol. 2011; 69(4):602–618. [PubMed: 21520230]
10. Sherman LS, Back SA. A ‘GAG’ reflex prevents repair of the damaged CNS. Trends Neurosci. 2008; 31(1):44–52. [PubMed: 18063497]
11. Preston M, Sherman LS. Neural stem cell niches: roles for the hyaluronan-based extracellular matrix. Front Biosci (Schol Ed). 2011; 3:1165–1179. [PubMed: 21622263]
12. Back SA, Tuohy TM, Chen H, Wallingford N, Craig A, et al. Hyaluronan accumulates in demyelinated lesions and inhibits oligodendrocyte progenitor maturation. Nat Med. 2005; 11(9): 966–972. [PubMed: 16086023]
13. Struve J, Maher PC, Li YQ, Kinney S, Fehlings MG, et al. Disruption of the hyaluronan-based extracellular matrix in spinal cord promotes astrocyte proliferation. Glia. 2005; 52(1):16–24. [PubMed: 15892130]
14. Buser JR, Maire J, Riddle A, Gong X, Nguyen T, et al. Arrested pre-oligodendrocyte maturation contributes to myelination failure in premature infants. Ann Neurol. 2012; 71:93–109. [PubMed: 22275256]
15. Back SA, Kroenke CD, Sherman LS, Lawrence G, Gong X, et al. White matter lesions defined by diffusion tensor imaging in older adults. Ann Neurol. 2011; 70(3):465–76. [PubMed: 21905080]

16. Cargill R, Kohama SG, Struve J, Su W, Banine F, et al. Astrocytes in aged nonhuman primate brain gray matter synthesize excess hyaluronan. Neurobiol Aging. 2012; 33:830.e13–24. [PubMed: 21872361]
17. Jiang D, Liang J, Noble PW. Hyaluronan as an immune regulator in human diseases. Physiol Rev. 2001; 91(1):221–264. [PubMed: 21248167]
18. Soltés L, Mendichi R, Kogan G, Schiller J, Stankovska M, et al. Degradative action of reactive oxygen species on hyaluronan. Biomacromolecules. 2006; 7(3):659–668. [PubMed: 16529395]
19. Al'Qteishat A, Gaffney J, Krupinski J, Rubio F, West D, et al. Changes in hyaluronan production and metabolism following ischaemic stroke in man. Brain. 2006; 129(Pt 8):2158–2176. [PubMed: 16731541]
20. Sloane JA, Batt C, Ma Y, Harris ZM, Trapp B, et al. Hyaluronan blocks oligodendrocyte progenitor maturation and remyelination through TLR2. Proc Natl Acad Sci USA. 2010; 107(25): 11555–11560. [PubMed: 20534434]
21. Marret S, Delpech B, Delpech A, Asou H, Girard N, et al. Expression and effects of hyaluronan and of the hyaluronan-binding protein hyaluronectin in newborn rat brain glial cell cultures. J Neurochem. 1994; 62(4):1285–1295. [PubMed: 7510775]
22. Lee HG, Cowman MK. An agarose gel electrophoretic method for analysis of hyaluronan molecular weight distribution. Anal Biochem. 1994; 219(2):278–287. [PubMed: 8080084]
23. Botzki A, Rigden DJ, Braun S, Nukui M, Salmen S, et al. L-Ascorbic acid 6-hexadecanoate, a potent hyaluronidase inhibitor. X-ray structure and molecular modeling of enzyme-inhibitor complexes. J Biol Chem. 2004; 279(44):45990–45997. [PubMed: 15322107]
24. Baggenstoss BA, Weigel PH. Size exclusion chromatography-multiangle laser light scattering analysis of hyaluronan size distributions made by membrane-bound hyaluronan synthase. Anal Biochem. 2006; 352(2):243–251. [PubMed: 16476403]
25. Dissen GA, Lomniczi A, Neff TL, Hobbs TR, Kohama SG, et al. In vivo manipulation of gene expression in non-human primates using lentiviral vectors as delivery vehicles. Methods. 2009; 49(1):70–77. [PubMed: 19559089]
26. Atmuri V, Martin DC, Hemming R, Gutsol A, Byers S, et al. Hyaluronidase 3 (HYAL3) knockout mice do not display evidence of hyaluronan accumulation. Matrix Biol. 2008; 27(8):653–660. [PubMed: 18762256]
27. Zhang SC, Lundberg C, Lipsitz D, O'Connor LT, Duncan ID. Generation of oligodendroglial progenitors from neural stem cells. J Neurocytol. 1998; 27(7):475–489. [PubMed: 11246488]
28. Meyer MF, Kreil G, Aschauer H. The soluble hyaluronidase from bull testes is a fragment of the membrane-bound PH-20 enzyme. FEBS Lett. 1997; 413(2):385–388. [PubMed: 9280317]
29. Phelps B, Myles DG. The guinea pig sperm plasma membrane protein, PH-20, reaches the surface via two transport pathways and becomes localized to a domain after an initial uniform distribution. Dev Biol. 1987; 123(1):63–72. [PubMed: 3305112]
30. Jones MH, Davey PM, Aplin H, Affara NA. Expression analysis, genomic structure, and mapping to 7q31 of the human sperm adhesion molecule gene SPAM1. Genomics. 1995; 29(3):796–800. [PubMed: 8575780]
31. Jones R, Ma A, Hou ST, Shalgi R, Hall L. Testicular biosynthesis and epididymal endoproteolytic processing of rat sperm surface antigen 2B1. J Cell Sci. 1996; 109(Pt 10):2561–2570. [PubMed: 8923217]
32. Zheng Y, Martin-DeLeon PA. The mouse Spam1 gene: RNA expression pattern and lower steady-state level associated with the Rb(6. 16) translocation. Mol Reprod Dev. 1997; 46(3):252–257. [PubMed: 9041127]
33. Wang H, Zhan Y, Xu L, Feuerstein GZ, Wang X. Use of suppression subtractive hybridization for differential gene expression in stroke: discovery of CD44 gene expression and localization in permanent focal stroke in rats. Stroke. 2011; 32(4):1020–1027. [PubMed: 11283406]
34. Jenkins HG, Bachelard HS. Developmental and age-related changes in rat brain glycosaminoglycans. J Neurochem. 1988; 51(5):1634–1640. [PubMed: 3139839]
35. Jenkins HG, Bachelard HS. Glycosaminoglycans in cortical autopsy samples from Alzheimer brain. J Neurochem. 1988; 51(5):1641–1645. [PubMed: 3139840]

36. Suzuki K, Katzman R, Korey SR. Chemical studies on Alzheimer's Disease. J Neuropathol Exp Neurol. 1965; 24:211–224. [PubMed: 14280498]
37. Contreras EG, Gaete M, Sánchez N, Carrasco H, Larraín J. Early requirement of Hyaluronan for tail regeneration in Xenopus tadpoles. Development. 2009; 136(17):2987–2996. [PubMed: 19666825]
38. Fancy SP, Baranzini SE, Zhao C, Yuk DI, Irvine KA, et al. Dysregulation of the Wnt pathway inhibits timely myelination and remyelination in the mammalian CNS. Genes Dev. 2009; 23(13): 1571–1585. [PubMed: 19515974]
39. Feigenson K, Reid M, See J, Crenshaw EB 3rd, Grinspan JB. Wnt signaling is sufficient to perturb oligodendrocyte maturation. Mol Cell Neurosci. 2009; 42(3):255–265. [PubMed: 19619658]
40. Azim K, Butt AM. GSK3β negatively regulates oligodendrocyte differentiation and myelination in vivo. Glia. 2011; 59(4):540–553. [PubMed: 21319221]
41. Tawk M, Makoukji J, Belle M, Fonte C, Trousson A, et al. Wnt/beta-Catenin Signaling Is an Essential and Direct Driver of Myelin Gene Expression and Myelinogenesis. J Neurosci. 2011; 31(10):3729–3742. [PubMed: 21389228]
42. Termeer C, Benedix F, Sleeman J, Fieber C, Voith U, et al. Oligosaccharides of Hyaluronan activate dendritic cells via toll-like receptor 4. J Exp Med. 2002; 195(1):99–111. [PubMed: 11781369]
43. Taylor KR, Trowbridge JM, Rudisill JA, Termeer CC, Simon JC, et al. Hyaluronan fragments stimulate endothelial recognition of injury through TLR4. J Biol Chem. 2004; 279(17):17079–17084. [PubMed: 14764599]
44. Jiang D, Liang J, Fan Y, Yu S, Chen S, et al. Regulation of lung injury and repair by Toll-like receptors and hyaluronan. Nat Med. 2005; 11(11):1173–1179. [PubMed: 16244651]
45. Scheibner KA, Lutz MA, Boodoo S, Fenton MJ, Powell JD, et al. Hyaluronan fragments act as an endogenous danger signal by engaging TLR2. J Immunol. 2006; 177(2):1272–1281. [PubMed: 16818787]
46. Shimada M, Yanai Y, Okazaki T, Noma N, Kawashima I, et al. Hyaluronan fragments generated by sperm-secreted hyaluronidase stimulate cytokine/chemokine production via the TLR2 and TLR4 pathway in cumulus cells of ovulated COCs, which may enhance fertilization. Development. 2008; 135(11):2001–2011. [PubMed: 18434414]
47. Kim JS, Yeo S, Shin DG, Bae YS, Lee JJ, et al. Glycogen synthase kinase 3beta and beta-catenin pathway is involved in toll-like receptor 4-mediated NADPH oxidase 1 expression in macrophages. FEBS J. 2010; 277(13):2830–2837. [PubMed: 20528914]
48. Zhang P, Katz J, Michalek SM. Glycogen synthase kinase-3beta (GSK3beta) inhibition suppresses the inflammatory response to Francisella infection and protects against tularemia in mice. Mol Immunol. 2009; 46(4):677–687. [PubMed: 18929413]
49. Wang Y, Cheng X, He Q, Zheng Y, Kim DH, et al. Astrocytes from the contused spinal cord inhibit oligodendrocyte differentiation of adult oligodendrocyte precursor cells by increasing the expression of bone morphogenetic proteins. J Neurosci. 2011; 31(16):6053–6058. [PubMed: 21508230]
50. Mi S, Hu B, Hahm K, Luo Y, Kam Hui ES, et al. LINGO-1 antagonist promotes spinal cord remyelination and axonal integrity in MOG-induced experimental autoimmune encephalomyelitis. Nat Med. 2007; 13(10):1228–1233. [PubMed: 17906634]
51. Stern R, Jedrzejas MJ. Hyaluronidases: their genomics, structures, and mechanisms of action. Chem Rev. 2006; 106(3):818–839. [PubMed: 16522010]
52. Martin DC, Atmuri V, Hemming RJ, Farley J, Mort JS, et al. A mouse model of human mucopolysaccharidosis IX exhibits osteoarthritis. Hum Mol Genet. 2008; 17(13):1904–1915. [PubMed: 18344557]
53. Triggs-Raine B, Salo TJ, Zhang H, Wicklow BA, Natowicz MR. Mutations in HYAL1, a member of a tandemly distributed multigene family encoding disparate hyaluronidase activities, cause a newly described lysosomal disorder, mucopolysaccharidosis IX. Proc Natl Acad Sci USA. 1999; 96(11):6296–6300. [PubMed: 10339581]

54. Jadin L, Wu X, Ding H, Frost GI, Onclinx C, et al. Skeletal and hematological anomalies in HYAL2-deficient mice: a second type of mucopolysaccharidosis IX? FASEB J. 2008; 22(12): 4316–4326. [PubMed: 18772348]

55. Baba D, Kashiwabara S, Honda A, Yamagata K, Wu Q, et al. Mouse sperm lacking cell surface hyaluronidase PH-20 can pass through the layer of cumulus cells and fertilize the egg. J Biol Chem. 2002; 277(22):30310–30314. [PubMed: 12065596]

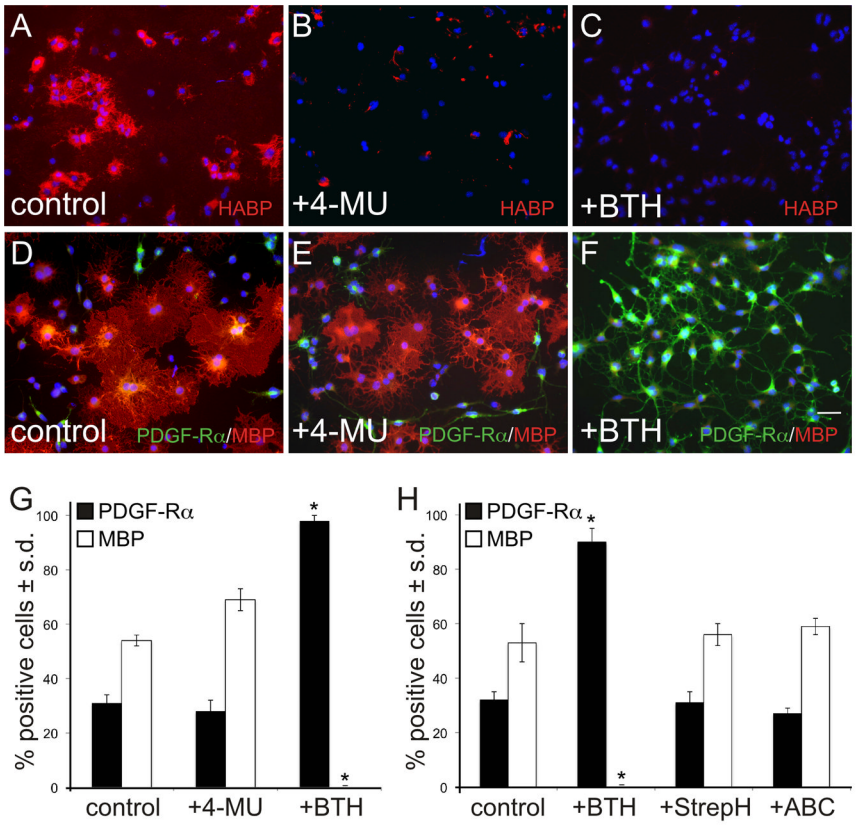

Figure 1.

Bovine testicular hyaluronidase inhibits OPC maturation, *in vitro*. OPCs were grown in pro-differentiation medium containing T3 and NAC. Control OPC cultures (A, D) were analyzed relative to cultures treated with the HA synthase inhibitor 4-MU (B, E), or with PH20 (C, F). After 96 hours, cultures were fixed and stained for the OL lineage markers MBP (red; to label mature OLs), PDGFR-α (green; to label OPCs), and DAPI (blue; to visualize cell nuclei). Panels A–C show representative levels of HA (as assayed using HABP histochemistry) for each treatment group. The total percentage of PDGFR-α+ and MBP+ cells are quantified in (G). PH20 treatment significantly inhibited OL maturation as shown by a decreased percentage of cells expressing MBP compared to controls (<0.5% vs. 54.1%), and an increased percentage of cells expressing PDGFR-α compared to controls (97.8% v. 30.9%). Inhibiting HA synthesis did not significantly alter OL maturation (E, G). (H) Quantification of OPC maturation in the presence of chondroitinase ABC ("ABC") or *Streptomyces*-derived hyaluronidase ("StrepH"). Unlike PH20, neither of these enzymes demonstrated any significant effect on OPC maturation. These experiments were performed 4 times with each data point assayed in triplicate wells. Scale bar = 10 μm. *p<0.0003.

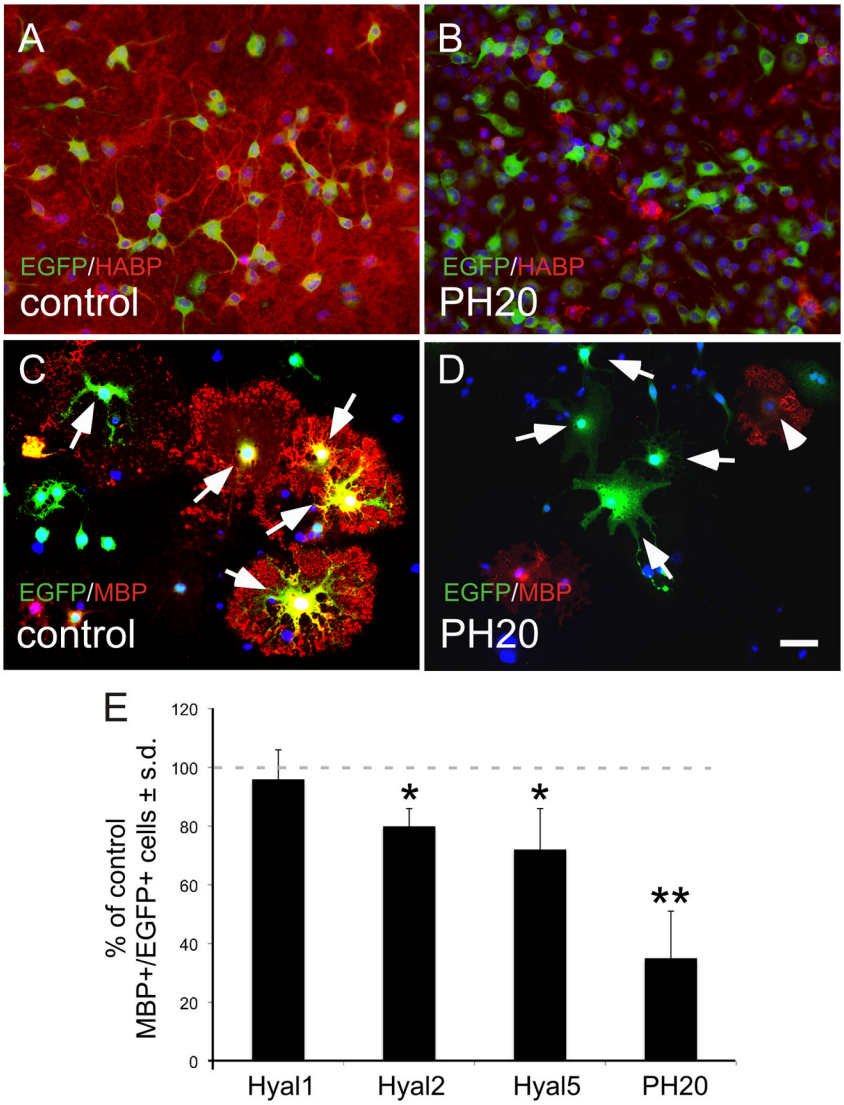

Figure 2.

Elevated expression of PH20, the soluble hyaluronidase in PH20, blocks OL maturation *in vitro*. OPCs were infected with lentiviruses carrying EGFP only (control; A, C), or viruses carrying EGFP plus *Hyal1*, *Hyal2*, *Hyal5* (not shown) or *PH20* (B, D). Cells were grown for 96 hours and stained for EGFP (green) and either HABP (A, B; red) or MBP (C, D; red). (E) Quantification of MBP expression by EGFP+ cells relative to cultures infected with the virus carrying EGFP alone. PH20 overexpression resulted in reduced HABP staining and inhibited OL maturation compared to cultures infected with only EGFP. HYAL2 overexpression partially inhibited OL maturation (78.48% of control). HYAL5 overexpression also partially inhibited OL maturation (70.08% of control). These experiments were performed 4 times with each data point assayed in triplicate wells. *$p<0.02$; **$p<0.0009$. Scale bar = 10 μm.

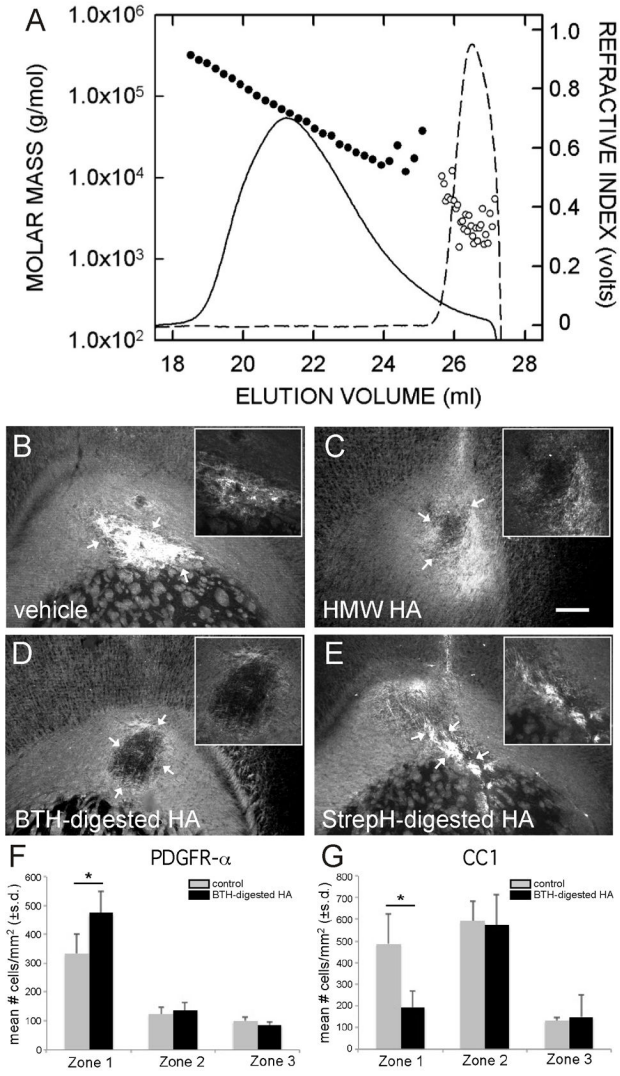

Figure 3.

PH20 digestion products of HA block remyelination. (A) HA samples were treated with BTH/PH20 (solid line and black circles) or StrepH (dashed line and white circles) and analyzed by SEC-MALLS to determine the amount (refractive index, solid and dashed lines) and the molar masses based on light scattering (black and white circles) of HA products present. The weight-average masses of the BTH/PH20 and StrepH samples were 63.9 ± 0.5 kDa and 2.4 ± 0.4 kDa, respectively. Overlap of the two digests was ≤ 2% (e.g. 98% of the BTH/PH20 products ranged from 5.5 to 227 kDa and 98% of the StrepH products were < 4.4 kDa). (B) Vehicle alone, (C) HMW HA (100μg/mL), (D) BTH/PH20-degraded HA (100μg/mL), or (D) StrepH degraded HA (100μg/mL) was stereotactically co-injected with lysolecithin into the corpus callsoum. Each HA preparation was re-injected without lysolecithin into demyelinated lesions 5 days later. Remyelination was determined by immunolabeling for MBP 8 days after lysolecithin injection. Arrows in B and E indicate the typical pattern of enhanced MBP immunoreactivity (white) in areas of apparent remyelination. Note that because of the broad dynamic range of the signal, areas of remyelination appear over-exposed. Insets show digitally enlarged images of lesions with reduced brightness and contrast, demonstrating the morphology within lesions. Arrows in C and D indicate regions of persistent lysolecithin-induced demyelination. This experiment

was performed 3 times. Scale bars = 250 μm. (F) Quantification of the density of PDGFR-α + cells within lesions (zone 1), at lesion borders (zone 2), and in adjacent unaffected white matter (zone 3). Note that there is an increase in PDGFR-α+ cells within lesions that is enhanced by PH20-digested HA. *p<0.002. (G) Quantification of CC1+ cells in the different zones of demyelinated lesions. Note that CC1+ cells increase in number both within lesions and at lesion borders. PH20-digested HA significantly inhibits the maturation of these mature OLs within the lesion. *p<0.001.

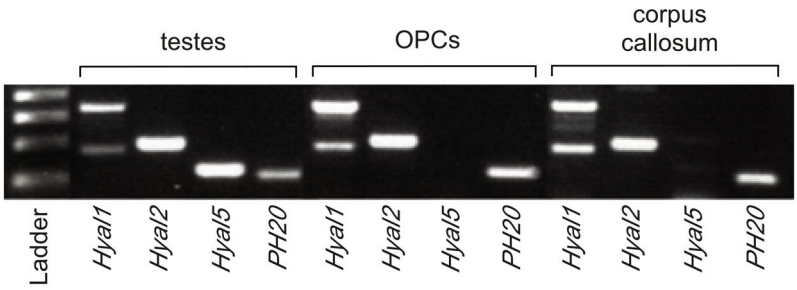

Figure 4.

OPCs express multiple hyaluronidases. Total mRNA was isolated from mouse testes (as a positive control), OPCs and adult mouse corpus callosum, reverse transcribed and subjected to RT-PCR. OPCs express *Hyal1*, *Hyal2* and *PH20* but not the testes-specific *Hyal5*. The same patterns of hyaluronidase expression were found in the corpus callosum.

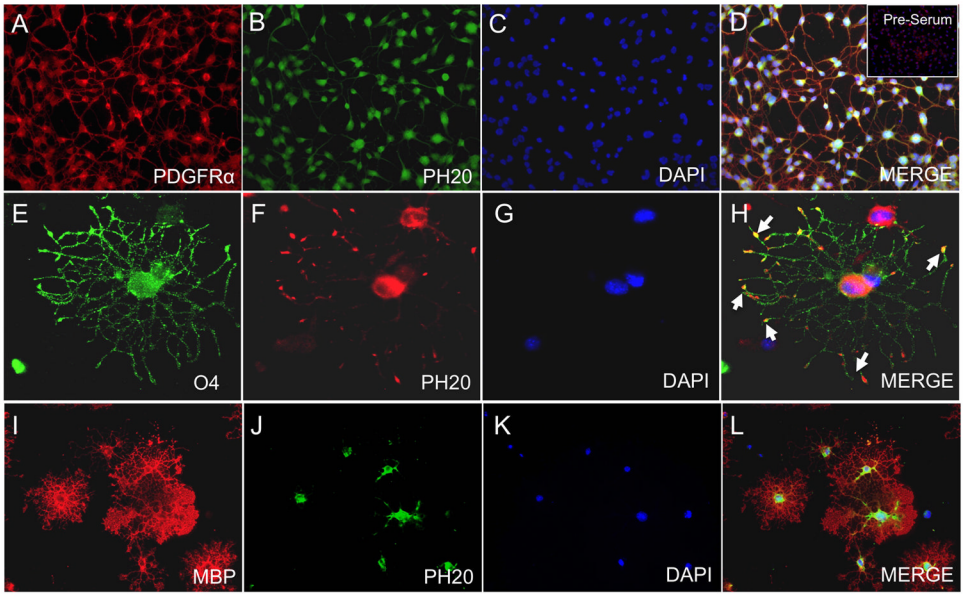

Figure 5.

PH20 expression is differentially localized on proliferating OPCs compared to mature OLs *in vitro*. PH20 expression was confirmed by immunocytochemistry in OPCs (A–D), pre-oligodendrocytes (E–H), and in maturing OLs (I–L). In OPCs, PH20 expression (B, green) was seen in cell bodies and processes of PDGFR-α+ OPCs (A, red). Inset in panel (D) shows lack of staining in OPCs incubated with preimmune serum. (F) Distribution of PH20 (red) in an O4+ (E; green) cell. PH20 was expression is observed in the tips of O4+ processes (arrows; H). PH20 expression became confined to the cell body (J; green) of MBP + OLs (I; red). DAPI (blue) was used to identify cell nuclei. Merged images are shown in D, H and L.

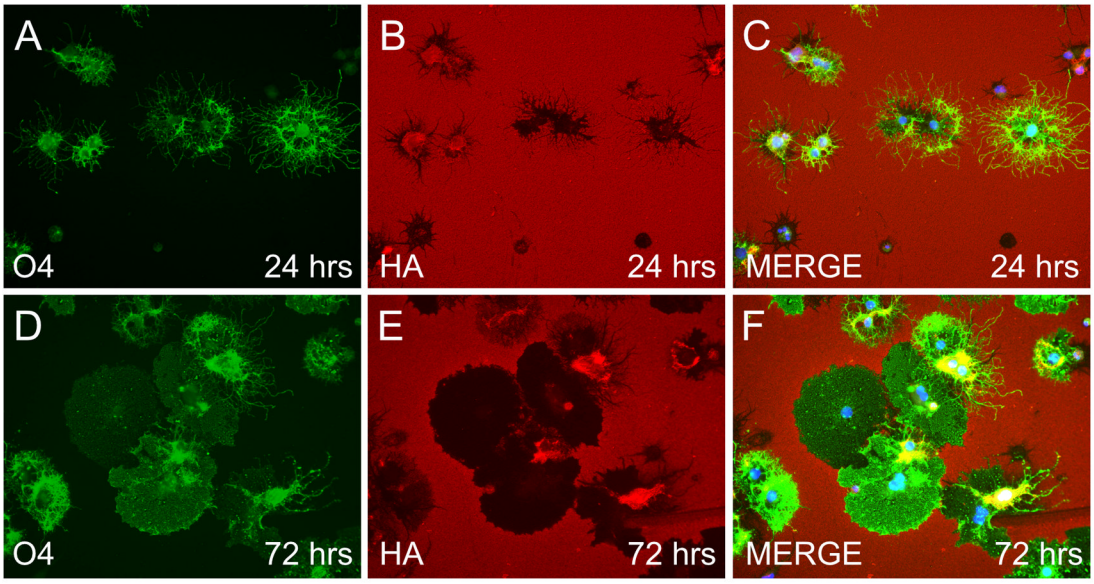

Figure 6.

OPCs and later OL stage cells degrade HA. OPCs grown in the presence of T3 and NAC were plated onto coverslips coated with HMW HA, allowed to mature for 24 (A–C) or 72 (D–F) hours and stained with O4 (green), HABP (red) and DAPI (blue). Pronounced degradation of HA, as assayed by loss of HABP staining, was seen around cell bodies and the extensive O4+ processes (A–C) at 24 hours. By 72 hours substantial degradation of HA was also observed (D–F) in areas corresponding to the presence of O4+ membranes that resemble myelin sheets. Note that HA was preserved around many OPC and mature OL cell bodies.

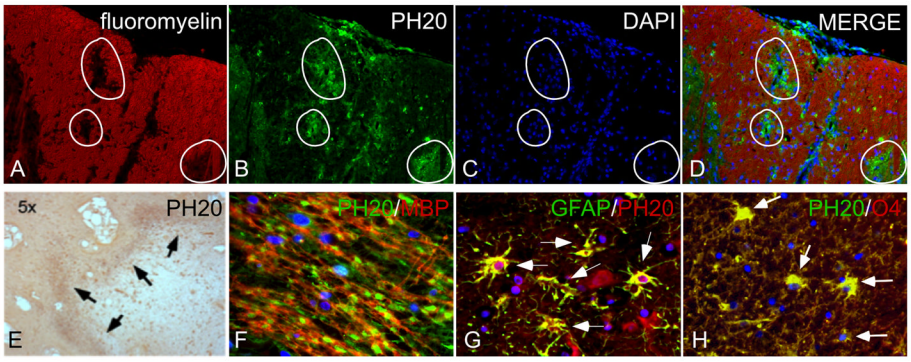

Figure 7.

PH20 expression in demyelinated lesions. (A–D) Sections of lumbar spinal cord from mice with EAE, 21 days post-inoculation with MOG. PH20 immunoreactivity (green; B, D) was elevated in areas where there was demyelination (indicated by white circles), identified by loss of fluoromyelin (red) staining (A, D) and increased DAPI labeling (C, D). Merged image is shown in D. (E–H) PH20 is also expressed by glial cells at the borders of chronic, cortical MS patient lesions. PH20 immunoreactivity was enriched at the borders of lesions (arrows, E). Numerous cells expressed PH20 in the lesion borders (F; MBP, red; PH20, green). (G) Double-labeling of MS patient lesion with antibodies against PH20 (red) and GFAP (green). (H) Double-labeling of MS patient lesions with PH20 (green) and O4 (red). Images in A–E are 5x; images in F–H are 40x. Sections were counterstained with DAPI (blue) to label cell nuclei.

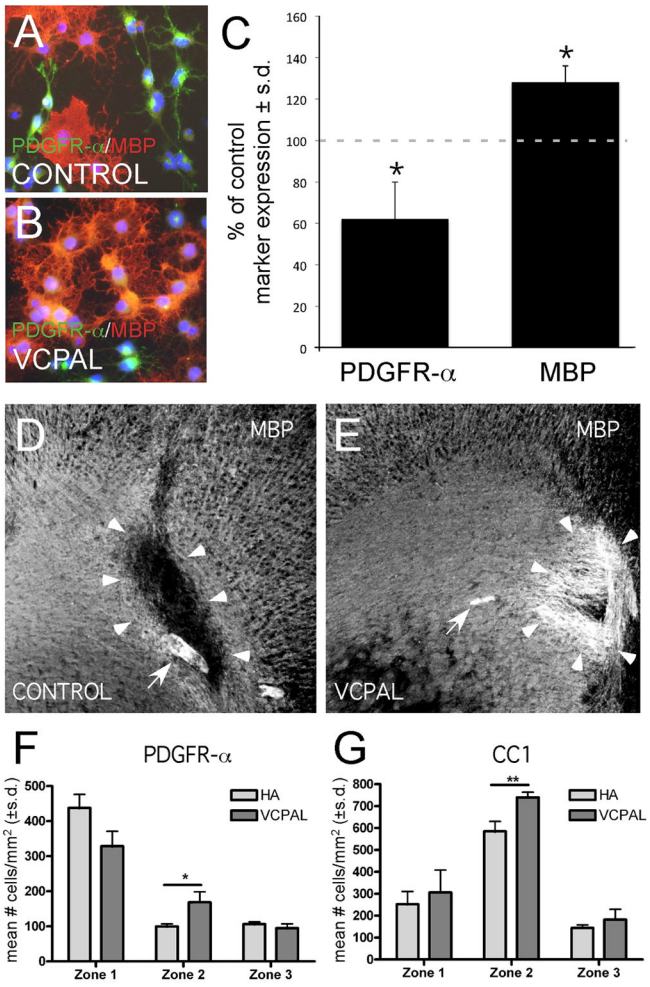

Figure 8.

Inhibiting endogenous hyaluronidase activity promotes OL maturation *in vitro* and remyelination *in vivo*. (A) OPCs were grown in OL differentiation medium alone or (B) with 25μM VCPAL for 72–96 hours and stained with MBP, PDGFR-α and DAPI. Total MBP+ and PDGFR-α+ cells are quantified in (C). Consistent with the hypothesis that hyaluronidases expressed by OPCs generate HA digestion products that inhibit OL maturation, blocking HYAL activity with VCPAL increased the total percentage of MBP+ cells compared to controls (69% vs. 54% p= 0.005) while decreasing the total percentage of PDGFR-α+ cells (19% v. 30% in control, p=0.02). (D, E) MBP immunoreactivity (white) of lysolecithin lesions treated with HMW HA and vehicle (D) or HMW HA with 25 μM VCPAL (E). Arrowheads indicate the borders of the demyelinated lesion in D and the area of remyelination in E; arrows indicate tissue areas with autofluorescence. Scale bar = 250 μm. (F) Quantification of PDGFR-α+ cells within lesions (zone 1), at lesion borders (zone 2) and in adjacent unaffected white matter (zone 3). Note that there was a trend within lesions for a reduction in the number of PDGFR-a+ cells. Within the lesion border, there was a significant increase in OL progenitors. (G) Quantification of CC1+ cells within the different lesion zones. The apparent recruitment of OL progenitors in the lesion border (F) was accompanied by an increased density of CC1+ mature OLs in the lesion border in G (and a similar trend within lesions). **p<0.001.

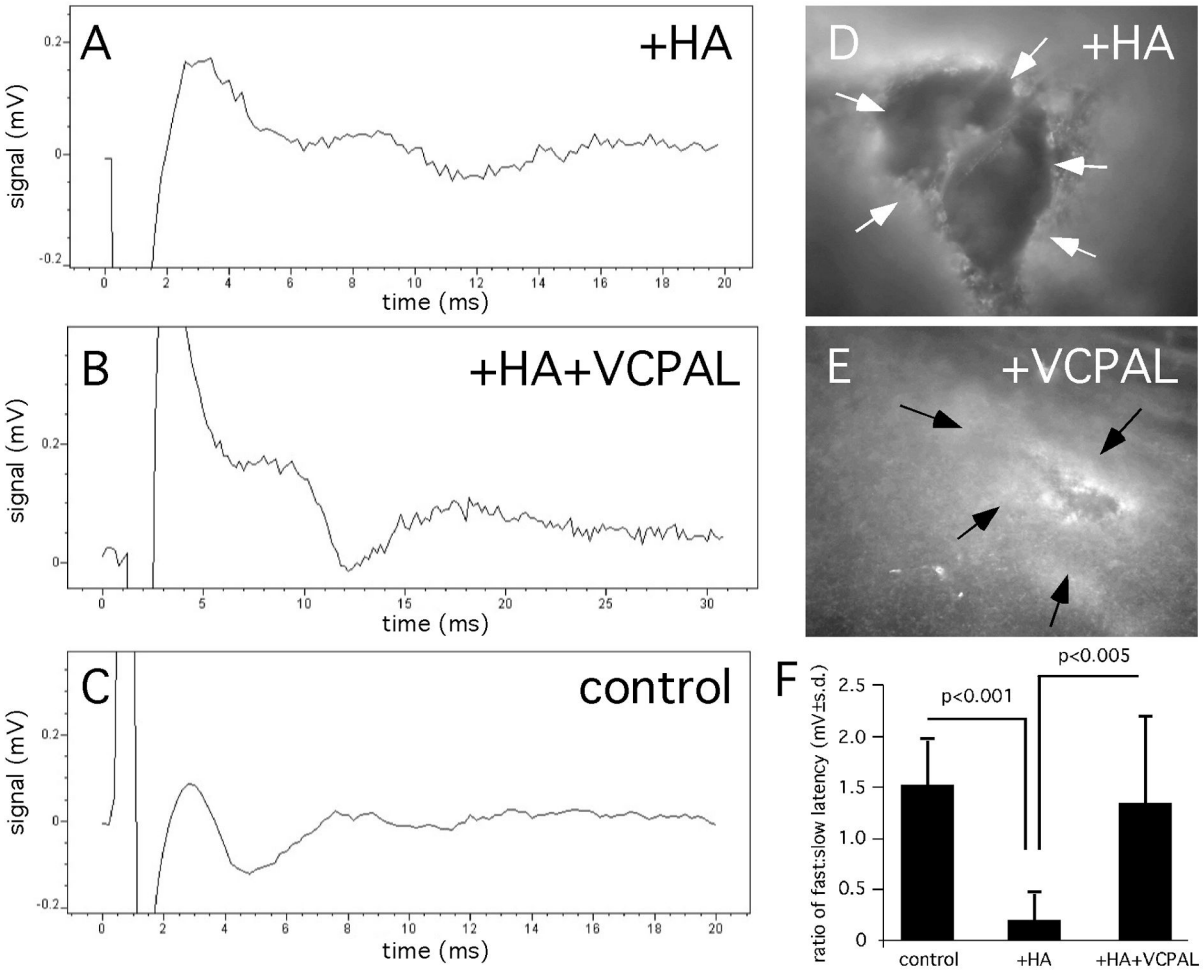

Figure 9.

CAP recordings of lysolecithin-induced demyelinating lesions treated with VCPAL or vehicle. (A–C) Raw traces of recordings of slices from (A) a lesion treated with vehicle and HA; (B) a lesion treated with HA and 25 μM VCPAL; and (C) the uninjected contralateral hemisphere of the animal in A. Following recording, slices were fixed in paraformaldehyde then stained as whole-mounts with an anti-MBP antibody (white). (D) A slice from an animal injected with HA and vehicle. (E) A slice from an animal injected with HA and VCPAL. (F) Quantification of the ratios of averaged recordings of fast and slow latencies. Note that slices treated with VCPAL demonstrated significant recovery of fast latency transduction.